Science Signaling
AAAS

www.sciencesignaling.org/cgi/content/full/11/521/eaam8858/DC1

Supplementary Materials for

TSLP signaling in CD4$^+$ T cells programs a pathogenic T helper 2 cell state

Yrina Rochman,* Krista Dienger-Stambaugh, Phoebe K. Richgels, Ian P. Lewkowich, Andrey V. Kartashov, Artem Barski, Gurjit K. Khurana Hershey, Warren J. Leonard, Harinder Singh*

*Corresponding author. Email: yrina.rochman@cchmc.org (Y.R.); harinder.singh@cchmc.org (H.S.)

Published 13 March 2018, *Sci. Signal.* **11**, eaam8858 (2018)
DOI: 10.1126/scisignal.aam8858

The PDF file includes:

Fig. S1. TSLP promotes T_H2 cell differentiation without affecting the survival or proliferation of activated CD4$^+$ T cells.
Fig. S2. TSLP enhances IL-4Rα abundance and promotes T_H2 cell differentiation in synergy with IL-4.
Fig. S3. Comparative transcriptional analysis of $T_H2^{IL\text{-}4}$ and T_H2^{TSLP} cells.
Fig. S4. JAK2 inhibitor II selectively blocks the TSLP-mediated activation of STAT5.
Fig. S5. Comparative chromatin analysis of $T_H2^{IL\text{-}4}$ and T_H2^{TSLP} cells.
Fig. S6. TSLP-responsive CD4$^+$ T cells, sensitized in vivo, manifest enhanced production of T_H2 cytokines.
Legends for tables S1 to S5
Table S6. Primers for PCR.
Table S7. Primers and probes for ChIP-DNA H3K27ac.

Other Supplementary Material for this manuscript includes the following:
(available at www.sciencesignaling.org/cgi/content/full/11/521/eaam8858/DC1)

Table S1 (Microsoft Excel format). Quantitative analysis of IL-13–positive CD4$^+$ T cells and the amounts of secreted IL-5 and IL-13.
Table S2 (Microsoft Excel format). RNA-seq analysis of the gene expression profiles of $T_H2^{IL\text{-}4}$ and T_H2^{TSLP} cells compared to that of T_H0 cells.

Table S3 (Microsoft Excel format). RNA-seq analysis of gene expression clusters and pathways in T_H0, T_H2, and T_H2^{TSLP} cells.
Table S4 (Microsoft Excel format). RNA-seq analysis of the gene expression profile of T_H2^{TSLP} cells compared to that of $T_H2^{IL\text{-}4}$ cells.
Table S5 (Microsoft Excel format). H3K27ac ChIP-seq tag density coordinates, 2.5-kb intervals around peak centers for shared peaks or peaks specific for T_H2 and T_H2^{TSLP} cells.

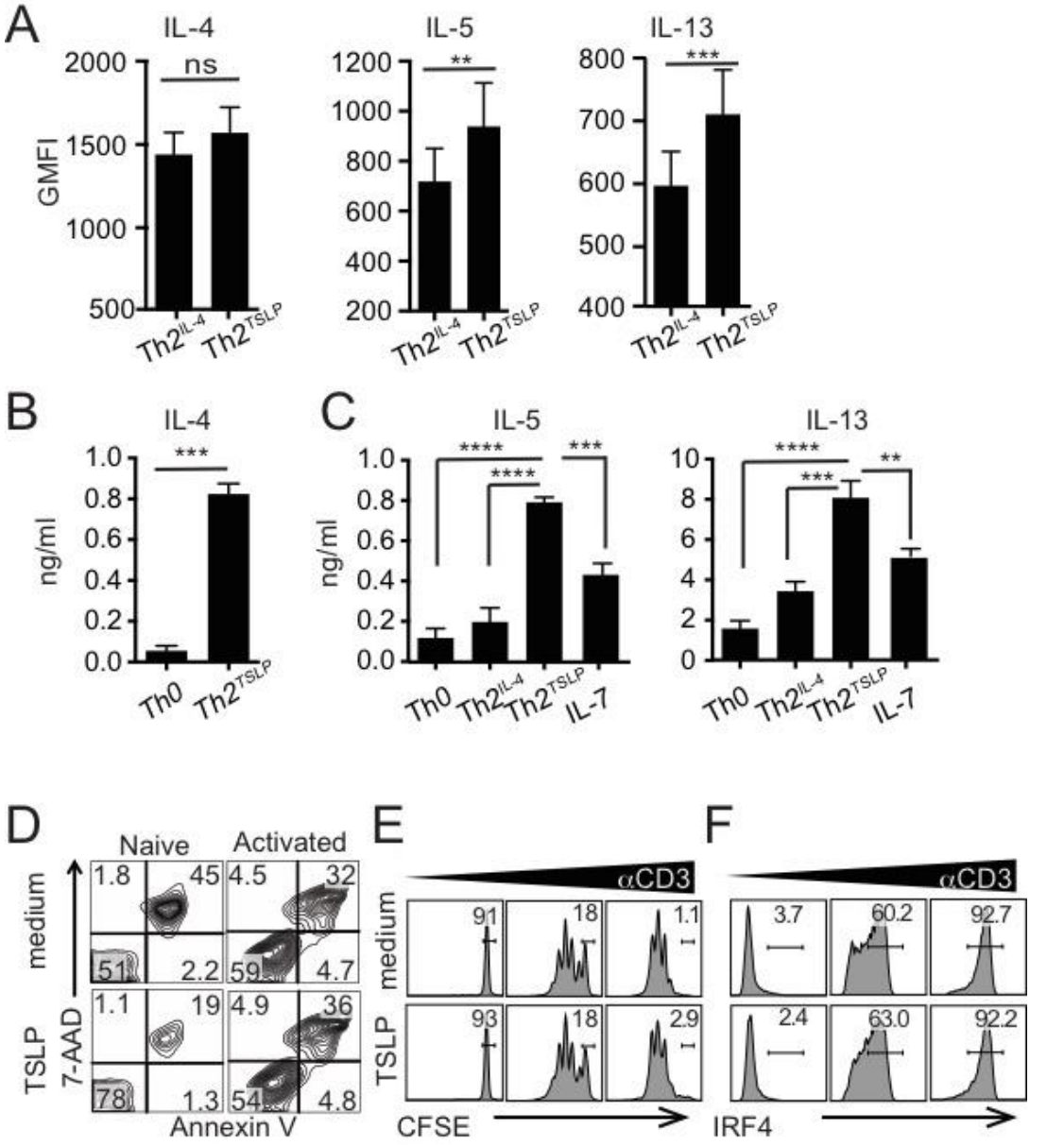

Fig. S1. TSLP promotes T_H2 cell differentiation without affecting the survival or proliferation of activated CD4$^+$ T cells. (**A** to **C**) Naïve CD4$^+$ T cells were activated as described in Fig. 1A. (A) Intracellular presence of the indicated cytokines in T_H2 or T_H2^{TSLP} cells after gating on IL-4–, IL-5–, or IL-13–positive cells. Data are means ± SEM of 10 experiments (for IL-4 and IL-13) or eight experiments (for IL-5). (B) The amounts of IL-4 (n = 3 experiments) and (C) IL-5 and IL-13 (n = 5 experiments) that were secreted by the indicated cells were determined by ELISA. Data are means ± SEM. Data were analyzed by paired *t* test (A and B) or one-way ANOVA (C). *$P \leq 0.05$, **$P \leq 0.01$, ***$P \leq 0.001$, ****$P \leq 0.0001$. (**D**) Unstimulated naïve CD4$^+$ T cells or those activated with a mixture of antibodies against CD3, CD28, and IFN-γ in the absence or presence of TSLP for 3 days were assessed for survival by flow cytometry using 7-AAD and annexin V. (**E**) Proliferation of cells was analyzed on day 3 using a CFSE dilution assay and varying doses of antibody against CD3 (0.2, 1 and 5 μg/ml) in the presence of anti-CD28 and anti-IFN-γ antibodies in the presence or absence of TSLP. (**F**) Detection of intracellular IRF4 on day 1 after CD4$^+$ T cell activation for cells treated as described in (E) Data in (D) to (F) are representative or three experiments.

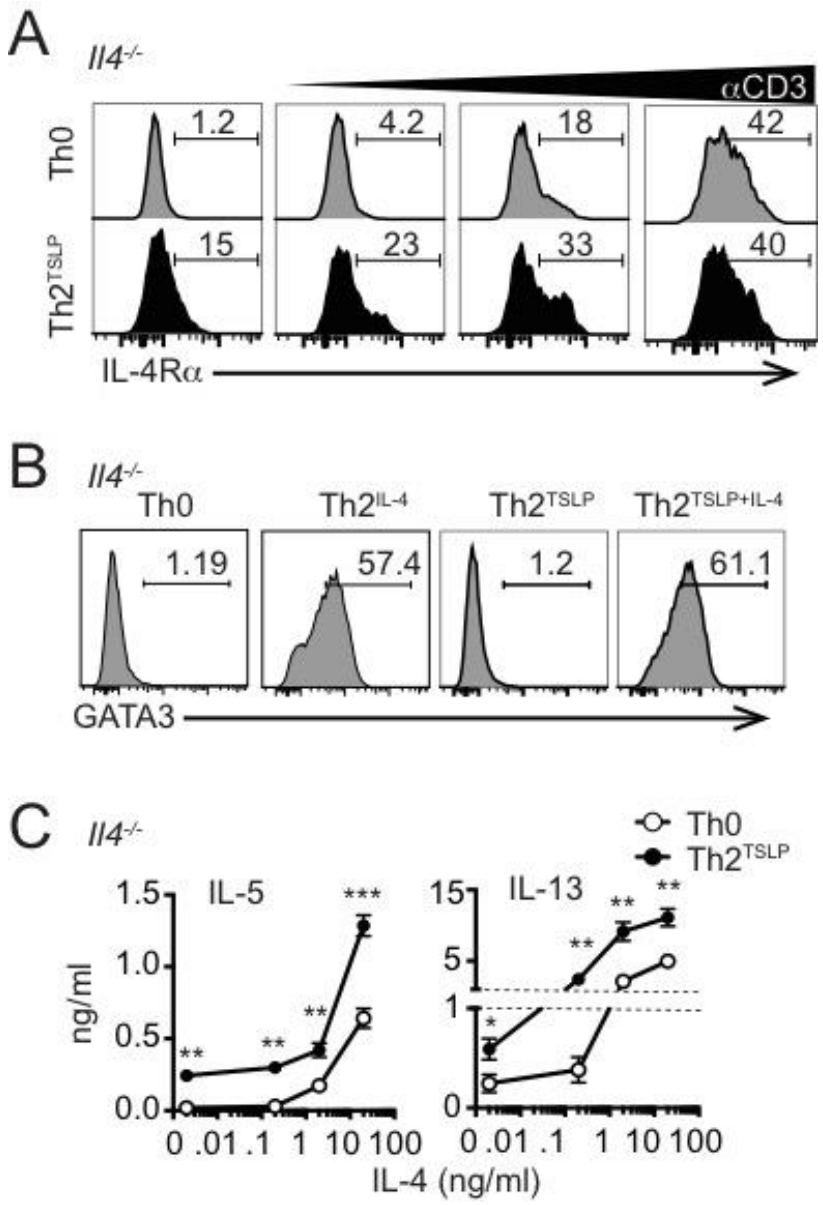

Fig. S2. TSLP enhances IL-4Rα abundance and promotes T_H2 cell differentiation in synergy with IL-4. (**A** to **C**) Naïve *Il4*$^{-/-}$ CD4$^+$ T cells were activated with antibodies against CD3, CD28, and IFN-γ in the presence or absence of TSLP and IL-4, as indicated. (A) Analysis of IL-4Rα abundance after 20 hours of T cell activation with varying doses of anti-CD3 (0.2, 1 and 5 μg/ml). Percentages of IL-4Rα$^+$ cells are indicated. (B) Percentages of GATA3$^+$ CD4$^+$ T cells on day 1 after the activation of naïve *Il4*$^{-/-}$ CD4$^+$ T cells with antibodies against CD3, CD28, and IFN-γ in the presence of the indicated cytokines. Data in (A and B) are representative one of four independent experiments. (C) The concentrations of IL-5 and IL-13 secreted by *Il4*$^{-/-}$ CD4$^+$ T cells upon activation in the absence or presence of TSLP and the indicated concentrations of IL-4 were determined on day 3. Data are means ± SEM of four experiments and were analyzed by one-way ANOVA. *$P \leq 0.05$, **$P \leq 0.01$, ***$P \leq 0.001$.

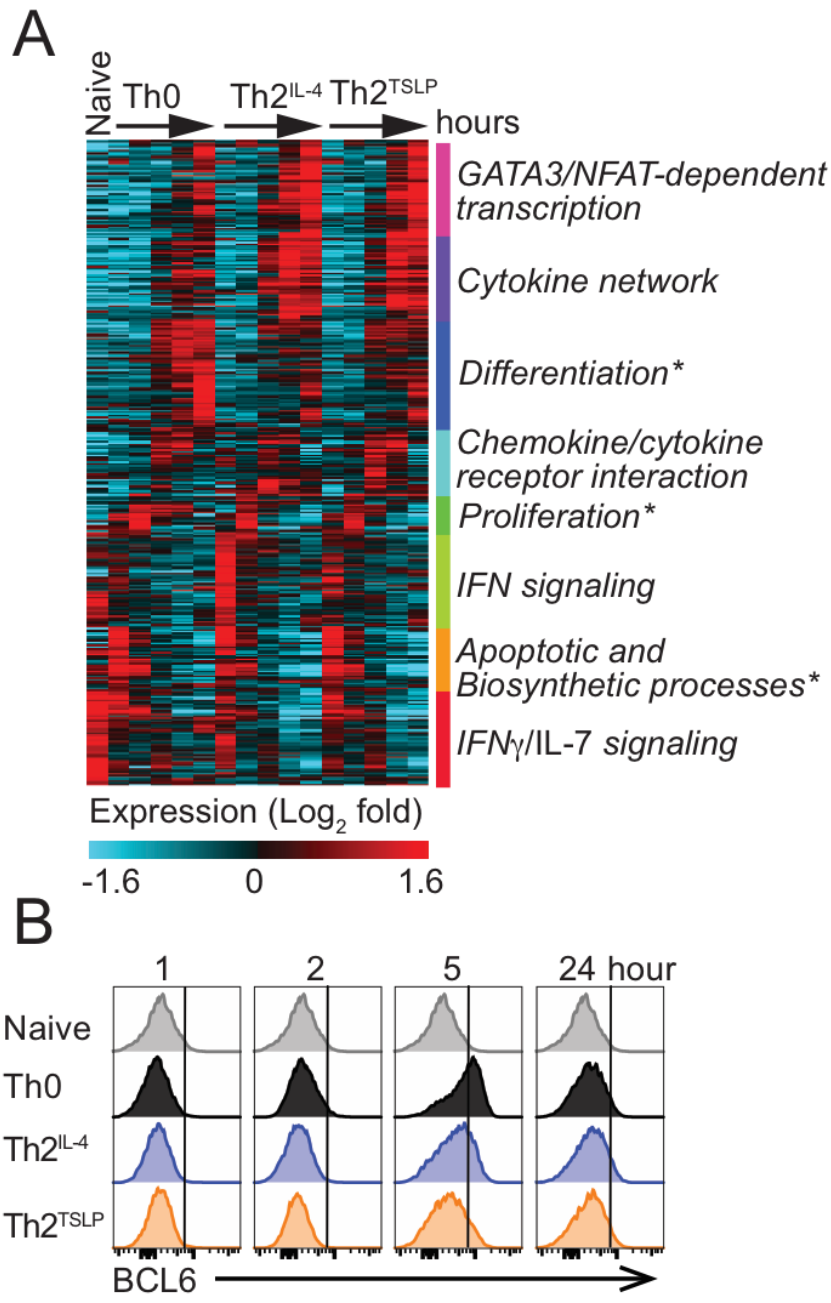

Fig. S3. Comparative transcriptional analysis of $T_H2^{IL\text{-}4}$ and T_H2^{TSLP} cells. (**A**) Naïve CD4$^+$ T cells were activated for 0, 2, 6, 24, 48, or 72 hours with antibodies against CD3, CD28, and IFN-γ in the absence or presence of IL-4 or TSLP and then were analyzed by RNA-Seq. The heat map displays pathway analysis for 377 differentially expressed genes (DEGs) based on comparison with T_H0 cells. Biological processes (marked with an asterisk) and pathways were assigned with ToppGene *(52)*. (**B**) Naïve CD4$^+$ T cells were activated with antibodies against CD3, CD28, and IFN-γ in the presence or absence of IL-4 or TSLP and the percentage of BCL6$^+$ CD4$^+$ T cells was measured by flow cytometry. A summary of data from multiple experiments is shown in Fig. 3D.

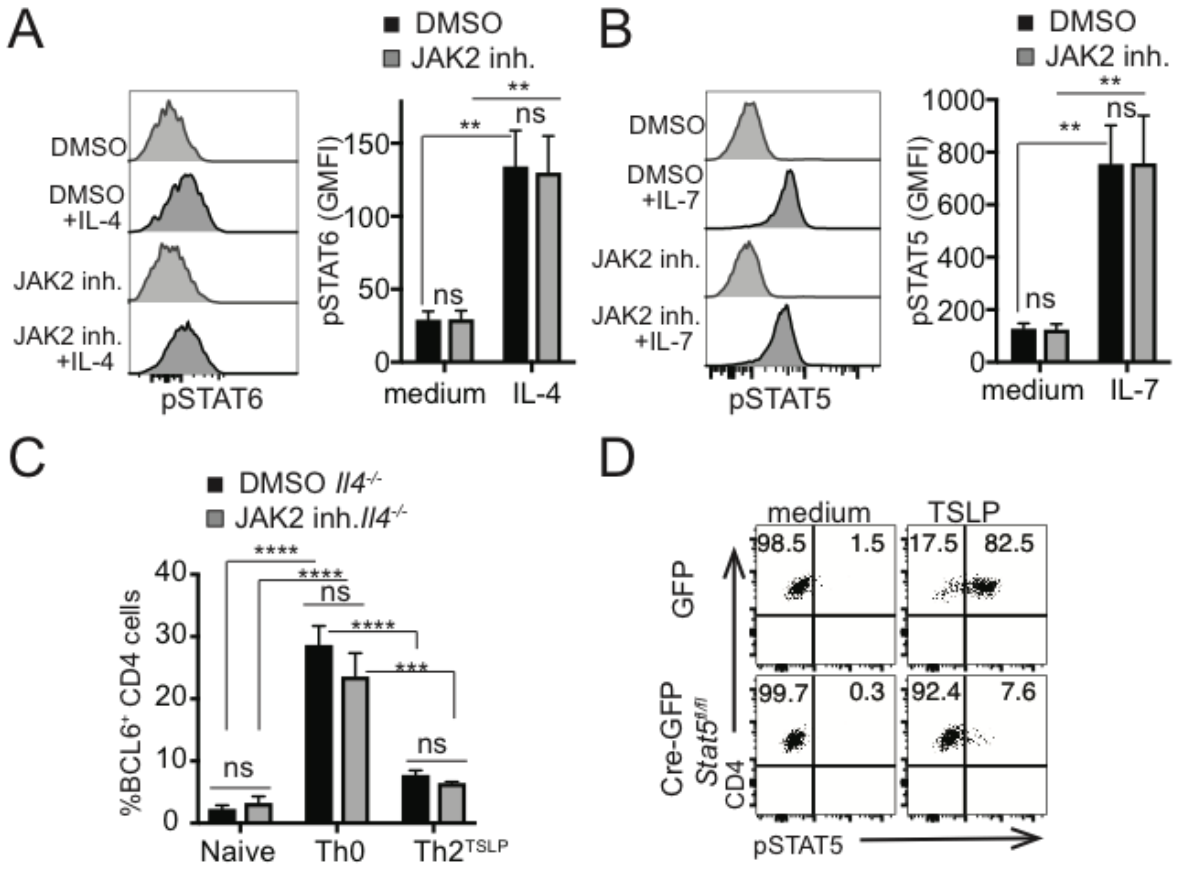

Fig. S4. JAK2 inhibitor II selectively blocks the TSLP-mediated activation of STAT5. (**A** and **B**) Naïve *Il4*$^{-/-}$ CD4^{+} T cells were pre-incubated for 1 hour with DMSO or 50 μM JAK2 inhibitor II (JAK2 inh.). Cells were left unstimulated or stimulated with IL-4 (A) or IL-7 (B) for 15 min. Phosphorylation of STAT6 (A) and STAT5 (B) was analyzed by flow cytometry. Left: Representative histograms used to calculate GMFI. Right: Quantitative data pooled from five independent experiments. (**C**) Naïve CD4^{+} T cells were unstimulated or activated with antibodies against CD3, CD28, and IFN-γ in the presence of DMSO or JAK2 inhibitor II with or without TSLP for 6 hours. BCL6 abundance was analyzed by flow cytometry. Data are from three experiments. (**D**) Naïve *Stat5a/5b*$^{fl/fl}$ CD4^{+} T cells were pre-activated and infected with GFP or Cre-GFP retroviruses as shown in Fig. 4C. Flow cytometry was used to analyze pSTAT5 in GFP-sorted cells after 15 min of stimulation with TSLP. Quantitative data in (A) to (C) are means ± SEM and were analyzed by ANOVA. $^{**}P \leq 0.01$, $^{***}P \leq 0.001$, $^{****}P \leq 0.0001$. ns, not significant.

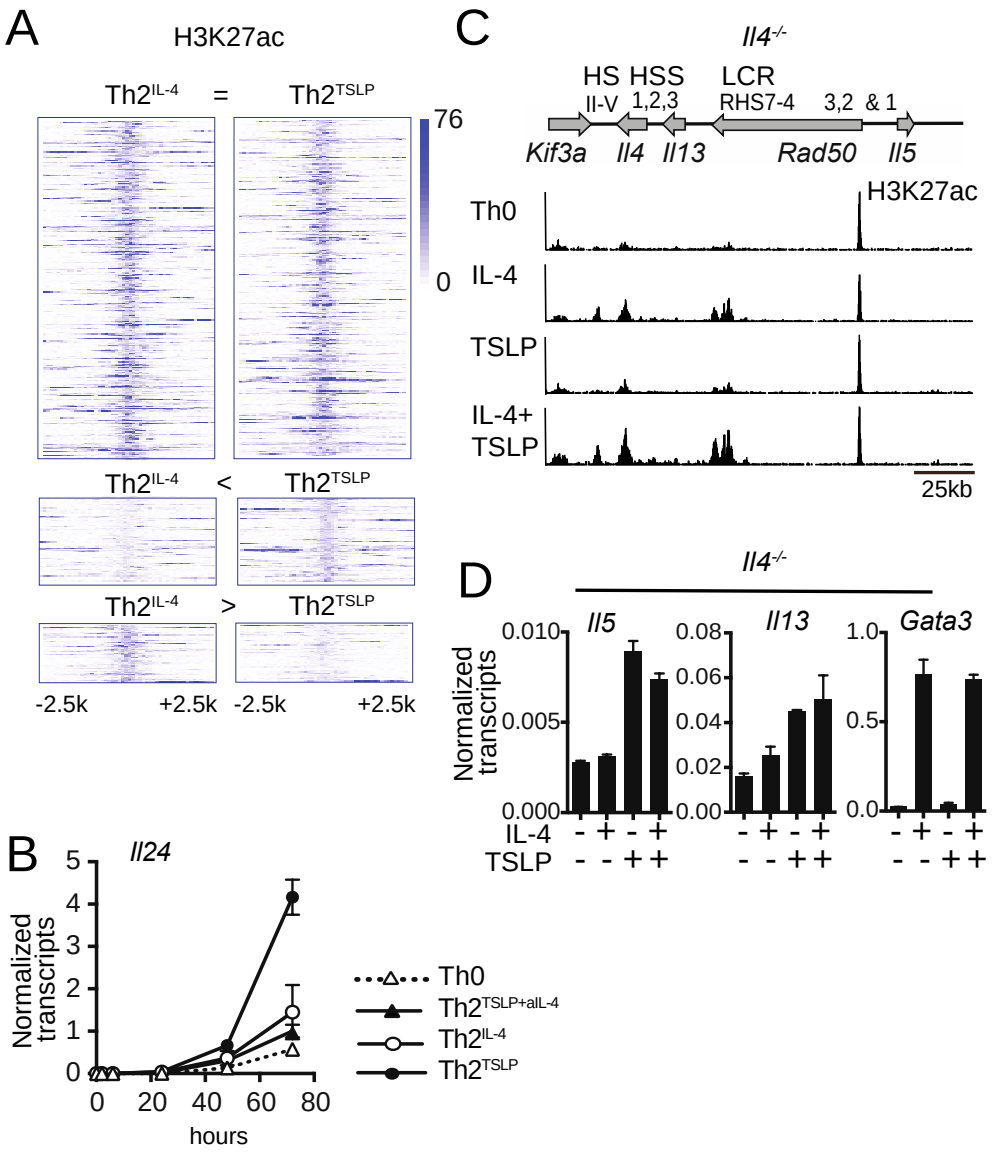

Fig. S5. Comparative chromatin analysis of $T_H2^{IL\text{-}4}$ and T_H2^{TSLP} cells. (**A**) Naïve CD4$^+$ T cells were activated as described in Fig. 1A in the presence or absence of IL-4 or TSLP for 3 days and then were analyzed by ChIP-Seq for H3K27ac. Heatmaps show H3K27ac ChIP-Seq tag density in 2.5-kb intervals around peak centers. Only those peaks that were present in $T_H2^{IL\text{-}4}$ or T_H2^{TSLP} cells but not in T_H0 cells are displayed. They comprised of 2611 shared peaks ($T_H2^{IL\text{-}4}$ or T_H2^{TSLP} cells), 90 unique peaks in T_H2^{TSLP} cells, and 60 unique peaks in $T_H2^{IL\text{-}4}$ cells. (**B**) Kinetics of *Il24* mRNA expression under the indicated differentiation conditions. Data are representative of three experiments. (**C** and **D**) Naïve *Il4*$^{-/-}$ cells were activated for 1 day in the presence of TSLP, IL-4, or both. ChIP-Seq analysis of H3K27ac at T_H2 cytokine loci (C) was performed and the mRNA abundance for indicated genes were measured by qPCR in the same experiment (D).

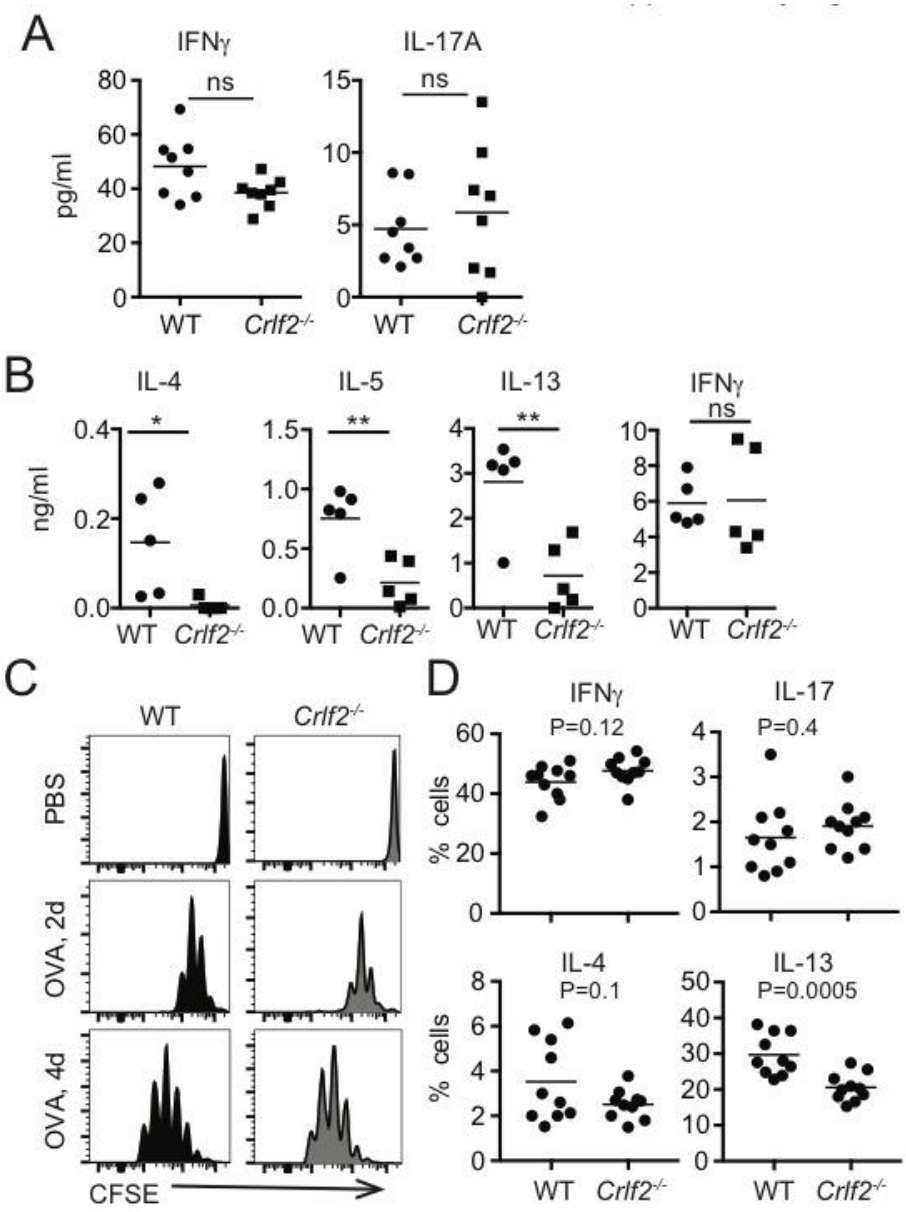

Fig. S6. TSLP-responsive CD4⁺ T cells, sensitized in vivo, manifest enhanced production of T_H2 cytokines. (**A**) WT or *Crlf2*$^{-/-}$ CD4$^+$ T cells were adoptively transferred into *Tcra*$^{-/-}$ mice, as detailed in Fig. 7. The amounts of IFN-γ and IL-17A in BAL fluid were determined. Data are means ± SEM of eight mice per group and were analyzed by two-tailed, unpaired *t* test; ns, not significant. (**B**) *Tcra*$^{-/-}$ mice were reconstituted with WT or *Crlf2*$^{-/-}$ CD4$^+$ T cells for five weeks and then administrated 100 μg of OVA with ALUM. On day 7**,** CD4$^+$ T cells were purified from spleens and restimulated in vitro with irradiated splenocytes loaded with 100 μg of OVA for 3 days. Data are representative of two experiments with five mice per group. Data are means ± SEM. *$P \leq 0.05$ and **$P \leq 0.01$ by two-tailed, unpaired *t* test. (**C** and **D**) WT or *Crlf2*$^{-/-}$ naïve CD4$^+$ T cells were transferred into *Crlf2*$^{-/-}$ mice that were treated with OVA and ALUM on the same day. (C) CD4$^+$ T cells were labeled with CFSE before adoptive transfer and their proliferation was evaluated. (D) On day 7, CD4$^+$ T cells were purified from spleens and restimulated in vitro with irradiated splenocytes loaded with OVA for 3 days. The percentage of cytokine-producing cells is shown. Data are means ± SEM of 10 mice per group and were analyzed by two-tailed, unpaired *t* test.

Table S1. Quantitative analysis of IL-13–positive $CD4^+$ T cells and the amounts of secreted IL-5 and IL-13. See Fig. 2E and fig. S2C for experimental details.

Table S2. RNA-seq analysis of the gene expression profiles of $T_H2^{IL\text{-}4}$ and T_H2^{TSLP} cells compared to that of T_H0 cells. See fig. S3A for experimental details. This table includes a list of 377 genes differentially expressed in $T_H2^{IL\text{-}4}$ and T_H2^{TSLP} cells in comparison to T_H0 cells. Data are presented as $\log_2$ of the fold-change in expression.

Table S3. RNA-seq analysis of gene expression clusters and pathways in T_H0, T_H2, and T_H2^{TSLP} cells. See fig. S3A for experimental details. Labels are as follows: Clusters, includes gene names for each cluster; Pathways, shows the top five statistically significant pathways for each cluster with each *P* value; Biological processes, shows the top five statistically significant biological processes for each cluster with each *P* value.

Table S4. RNA-seq analysis of the gene expression profile of T_H2^{TSLP} cells compared to that of $T_H2^{IL\text{-}4}$ cells. See Fig. 3A for experimental details. This table shows 22 genes that were increased in expression in T_H2^{TSLP} cells and 112 genes that were increased in expression in $T_H2^{IL\text{-}4}$ cells. Data are presented as the $\log_2$ of the fold-change in gene expression between T_H2^{TSLP} cells and $T_H2^{IL\text{-}4}$ cells.

Table S5. H3K27ac ChIP-seq tag density coordinates, 2.5-kb intervals around peak centers for shared peaks or peaks specific for T_H2 and T_H2^{TSLP} cells. See fig. S5A for experimental details. This table includes the names of genes and their locations. Labels are as follows: Common, shows genes with increased H3K27ac in both $T_H2^{IL\text{-}4}$ and T_H2^{TSLP}cells (which are listed in the first set of fig. S5A). Th2 TSLP, are genes with increased H3K27ac in T_H2^{TSP} cells (see the second panel of fig. S5A); Th2, are genes with increased H3K27ac in $T_H2^{IL\text{-}4}$ cells (see third panel of fig. S5A).

Table S6. Primers for PCR.

Gene ID	Forward	Reverse
mBcl6	CCTGAGGGAAGGCAATATCA	GTTTAAGTGCAGGGGCCATT
mCsf2	AGATATTCGAGCAGGGTCTACG	TCCGCATAGGTGGTAACTTG
mEif3k (control)	CACAAGCCAAAGAGAATGCC	TGAGGGCTTTCAGCAGAATC
mGata3	GCACTACCTTTGCAATGCCT	AGGATGTCCCTGCTCTCCTT
mIl4	ATGGAGCTGCAGAGACTCTTTC	TGGACTCATTCATGGTGCAG
mIl5	ATGAGGCTTCCTGTCCCTAC	CCACGGACAGTTTGATTCTTC
mIl9	CTCTTGCCTGTTTTCCATCG	GTCTGGTTGCATGGCTTTTC
mIl13	TGTGTCTCTCCCTCTGACCC	GCCAGGTCCACACTCCATAC
mIl24	GCAGGTTCTGCGGAATGTCT	GTTGGCCAGAGTGGAGAATG
hIL4	CAGACATCTTTGCTGCCTCC	GCAGCGAGTGTCCTTCTCAT
hIL5	CTCTGAGGATTCCTGTTCCTG	CTTGCACAGTTTGACTCTCCAG
hIL13	TTGAGGAGCTGGTCAACATC	CTGTCAGGTTGATGCTCCATAC

Table S7. Primers and probes for ChIP-DNA H3K27ac. *Actb* was used as a positive control, whereas *Myh11* was used as a negative control.

Gene ID	Forward	Reverse	Probe
*Actb**	CACGCTAGGCGTAAAGTTGG	TTCGCTCTCTCGTGGCTAGT	AGTGATCCTCAGGACCC
Il4 promoter	GACTTTGGGGCCTTTCATTC	ATTTGTAGTGGGAGGGGACAG	CAGTGGTGTGTTTCCATGAAAACAGGA
Il5 downstream	AGAAAGGAAGGGAAGGGGAAAC	TCATGCCAACGACCTCAAAC	TTTGGACACTGTGGTGGGGCAGGGGGTGC
Il13 downstream	TTGCCCCAGACATTTCCTGG	AGGCTGCTCAAAGGAGAGATAG	AGGGGGCGTGTCTCCTCGGTCGGCCA
*Myh11***	TCATCCCCTCTTCATTCACC	ATATGCGGTGACCTGCTTTG	TCTGAGGGCGGTTGTGTTTAGCAAAG